



## Beyond connecting the dots: A multi-scale, multi-resolution approach to marine habitat mapping

Karin J. van der Reijden<sup>a,b,\*</sup>, Laura L. Govers<sup>a,c</sup>, Leo Koop<sup>d</sup>, Johan H. Damveld<sup>e</sup>, Peter M. J. Herman<sup>f</sup>, Sebastiaan Mestdagh<sup>g</sup>, Gerjan Piet<sup>h</sup>, Adriaan D. Rijnsdorp<sup>h,i</sup>, Grete E. Dinesen<sup>b</sup>, Mirjam Snellen<sup>d,j</sup>, Han Olf<sup>a</sup>

<sup>a</sup> Conservation Ecology Group, Groningen Institute for Evolutionary Life Sciences (GELIFES), University of Groningen, PO Box 11103, 9700 CC Groningen, the Netherlands

<sup>b</sup> DTU Aqua, National Institute of Aquatic Resources, Technical University of Denmark, Kemitorvet, DK-2800, Kongens Lyngby, Denmark

<sup>c</sup> Department of Coastal Systems, NIOZ Royal Netherlands Institute for Sea Research, PO Box 59, 1790 AB Den Burg, the Netherlands

<sup>d</sup> Acoustics Group, Faculty of Aerospace Engineering, Delft University of Technology, PO Box 5058, 2600 GB Delft, the Netherlands

<sup>e</sup> Water Engineering and Management, University of Twente, PO Box 217, 7500 AE Enschede, the Netherlands

<sup>f</sup> Marine and Coastal Systems, Deltares, Rotterdamseweg 185, PO Box 177, 2600 MH Delft, the Netherlands

<sup>g</sup> NIOZ Royal Netherlands Institute for Sea Research, Department of Estuarine & Delta Systems, PO Box 140, 4400 AC Yerseke, the Netherlands

<sup>h</sup> Wageningen Marine Research, PO Box 68, 1970 AB IJmuiden, the Netherlands

<sup>i</sup> Aquaculture and Fisheries Group, Wageningen University, PO Box 338, 6700 AH Wageningen, the Netherlands

<sup>j</sup> Department of Applied Geology and Geophysics, Deltares, 3508 AL Utrecht, The Netherlands

### ARTICLE INFO

#### Keywords:

Benthic faunal assemblages  
Demersal fisheries  
Hierarchical clustering  
Marine habitat mapping  
Marine Spatial Planning  
Physiotopes

### ABSTRACT

Conflicts of interests between economic and nature conservation stakeholders are increasingly common in coastal seas, inducing a growing need for evidence-based marine spatial planning. This requires accurate, high-resolution habitat maps showing the spatial distribution of benthic assemblages and enabling intersections of habitats and anthropogenic activities. However, such detailed maps are often not available because relevant biological data are scarce or poorly integrated. Instead, physiotope maps, solely based on abiotic variables, are now often used in marine spatial planning. Here, we investigated how pointwise, relatively sparse biological data can be integrated with gridded, high-resolution environmental data into informative habitat maps, using the intensively used southern North Sea as a case-study. We first conducted hierarchical clustering to identify discrete biological assemblages for three faunal groups: demersal fish, epifauna, and endobenthos. Using Random Forest models with high-resolution abiotic predictors, we then interpolated the distribution of these assemblages to high resolution grids. Finally, we quantified different anthropogenic pressures for each habitat. Habitat maps comprised a different number of habitats between faunal groups (6, 13, and 10 for demersal fish, epifauna, and endobenthos respectively) but showed similar spatial patterns for each group. Several of these 'fauna-inclusive' habitats resembled physiotopes, but substantial differences were also observed, especially when few (6; demersal fish) or most (13; epifauna) physiotopes were delineated. Demersal fishing and offshore wind farms (OWFs) were clearly associated with specific habitats, resulting in unequal anthropogenic pressure between different habitats. Natura-2000 areas were not specifically associated with demersal fishing, but OWFs were situated mostly inside these protected areas. We thus conclude that habitat maps derived from biological datasets that cover relevant faunal groups should be included more in ecology-inclusive marine spatial planning, instead of only using physiotope maps based on abiotic variables. This allows better balancing of nature conservation and socio-economic interests in continental shelf seas.

\* Corresponding author.

E-mail addresses: [k.j.van.der.reijden@rug.nl](mailto:k.j.van.der.reijden@rug.nl), [kjova@aqu.dtu.dk](mailto:kjova@aqu.dtu.dk) (K.J. van der Reijden).

<https://doi.org/10.1016/j.ecolind.2021.107849>

Received 7 October 2020; Received in revised form 26 May 2021; Accepted 26 May 2021

Available online 2 June 2021

1470-160X/© 2021 The Author(s). Published by Elsevier Ltd. This is an open access article under the CC BY license (<http://creativecommons.org/licenses/by/4.0/>).

## 1. Introduction

Continental shelf seas are subject to increasing anthropogenic activities, such as shipping (Sardain et al., 2019), sediment extraction (de Boer et al., 2011), offshore wind farms (OWFs; Grothe & Schnieders, 2011) and industrial fishing (Eigaard et al., 2017). Meanwhile, calls for effective marine conservation are increasing (Johnson et al., 2017), for example, in demanding the establishment of no-use marine protected areas (Costello & Ballantine, 2015). Ecology-inclusive marine spatial planning that balances the socio-economic and ecological interests can help to resolve current spatial conflicts of interest (Kaiser et al., 2016; White, Halpern, & Kappel, 2012). At present, anthropogenic activities are predominantly located in areas where they are most profitable (Grothe and Schnieders, 2011). However, to improve the balance between both socio-economic and conservation interests, ecological knowledge on, for instance, species abundance and diversity, community sensitivity, and ecosystem resilience should also be included in spatial zonation of anthropogenic activities. This requires accurate high-resolution maps that capture the spatial heterogeneity, extent, and biological characteristics of different marine habitats (Kaiser et al., 2016; Reiss et al., 2015). These can be translated into maps representing the uniqueness, diversity, vulnerability and resilience of local demersal assemblages and their relation to anthropogenic pressures (Cooper et al., 2019; Kaiser et al., 2016).

Biological sampling (through research-based trawls, cores, grabs, etc.) provides information on the spatial distribution of benthic assemblages. However, such sampling is very labour intensive and expensive. It furthermore is prone to methodological limitations in capture efficiency, site accessibility, and sampling of all biological strata (Beisiegel et al., 2017; Jørgensen et al., 2011), and to observer bias in taxonomic identification (Reiss et al., 2010). In addition, biological samples are by nature 'station-based' point samples and thus need interpolation to obtain full-coverage predictions of benthic assemblage distributions. Accuracy increases with better interpolation techniques (ICES, 2019a) and higher sampling resolution (Compton et al., 2013; Cooper et al., 2019).

Due to these difficulties of collecting and analysing biological data, high-resolution environmental ('abiotic') variables are often typically used instead. Variables as water temperature, bathymetric depth, salinity and sediment type are typically derived through combinations of remote sensing, modelling and point measurements, and often form the basis for habitat mapping processes. This includes the currently most commonly used habitat mapping approach: hierarchical classification schemes (Strong et al., 2019). These maps are structured in multiple (stacked) hierarchical 'levels'. Lower levels delineate broad habitat types based only on environmental factors, often combinations of bathymetry and sediment composition categories. The more detailed, higher levels subsequently divide these into more specific habitat types, based on additional environmental factors and/or station-based biological information (Galparsoro et al., 2012; Schiele et al., 2014; Strong et al., 2019). However, usage of these maps is often limited to the broad, low-level habitat types, so based on environmental variables only (Andersen et al., 2018; Galparsoro et al., 2012; ICES, 2020).

Here, we define maps that are exclusively based on environmental variables as 'physiotope maps', which are often seen as surrogates for benthic assemblage distributions (Huang et al., 2011; McArthur et al., 2010; Roland Pitcher et al., 2012; Vasquez et al., 2015). However, although benthic communities are strongly affected by environmental conditions, they typically are not defined by static environmental conditions alone (Galparsoro et al., 2012; Stevens and Connolly, 2004). Communities and environmental conditions can be heavily affected by biological processes like predation, competition, or ecosystem engineering effects (Jones et al., 1994; Menge and Sutherland, 1976), and can change under anthropogenic pressures, such as frequent bottom trawling (Kaiser, Ramsay, Richardson, Spence, & Brand, 2000). Moreover, the relevance of different environmental factors varies greatly

between spatial scales (Damveld et al., 2018; Lecours et al., 2015), differs between faunal groups (e.g. demersal fish versus endobenthos; Hewitt et al., 2015), and not all relevant environmental variables may be included in physiotope maps. Therefore, physiotope maps at best represent the required biological reality only partially.

Using the North Sea as a case-study, we here explore a novel approach to derive high-resolution habitat maps that combine low resolution, point-based biological data of three faunal groups with higher resolution key environmental variables. The resulting habitat maps were compared with physiotope maps to visualize the contribution of biological input data. In this, the role of fishing intensity as an anthropogenic environmental variable was studied and spatial associations of anthropogenic uses (fisheries, OWFs, Natura-2000 areas) with the identified habitats were quantified. We conclude with a discussion on our findings can improve ecology-inclusive marine spatial planning in coastal seas.

## 2. Methods

In our study we compare habitat maps based on biological samples, spatially interpolated using high-resolution environmental gradients with physiotope maps that are solely based on the same environmental gradients (Fig. 1). Sampled species abundances of three faunal groupings were separately clustered into assemblages with a hierarchical clustering. Environmental gradients were determined by reducing 21 environmental variables (Table 1) to less dimensions (main environmental gradients) using Principal Component Analysis (PCA). The point-wise assemblages were interpolated based on these main environmental gradients into full-coverage habitat maps. The resulting habitat maps were then compared to physiotope maps, which resulted from a clustering of the main environmental gradients exclusively, to investigate the added value of biological information in the habitat mapping exercise. We additionally studied the potential of fishing intensity as an explanatory, anthropogenic variable by performing the whole analysis twice: first with the 21 environmental variables, and then with the 21 environmental variables in combination with fishing intensity.

### 2.1. Study area

In this study, we focused on the offshore Central and Southern North Sea, defined by the International Council for the Exploration of the Sea (ICES) as subdivisions IVb and IVc (Fig. 2). To avoid any near-coastal effects of modelled parameters, the national territorial waters (12 nautical miles from shoreline) are excluded from the analysis.

### 2.2. Biotic data

#### 2.2.1. Demersal fish

We obtained demersal fish abundances from the annual North Sea Beam Trawl Survey (BTS). This survey samples demersal fishes with a beam trawl (8 m width, 4 cm mesh size), at relatively fixed stations throughout the North Sea (Fig. 3A) by performing 30-min hauls at 5 knots (covering  $\sim 0.037 \text{ km}^2$ ). All caught individuals were identified and counted (see ICES, 2009 for detailed methodology). We obtained all BTS-data from the DATRAS website for the years 2008–2015 (Millar et al., 2019). Only valid hauls with species recordings, a maximum distance of 10 km covered, and located within the study area were included. Species with missing abundances were removed, as were all non-fish species and species with recordings in  $< 5$  hauls. For each haul, we determined species density (in number per  $\text{m}^2$ ), using swept area ( $\text{m}^2$ ) as the product of beam width and track distance.

#### 2.2.2. Epifauna

For epifauna, we used the data collected in 2003 and 2004 by the internationally harmonized MAFCONS project (Managing Fisheries to Conserve Groundfish and Benthic Invertebrate Species Diversity) that

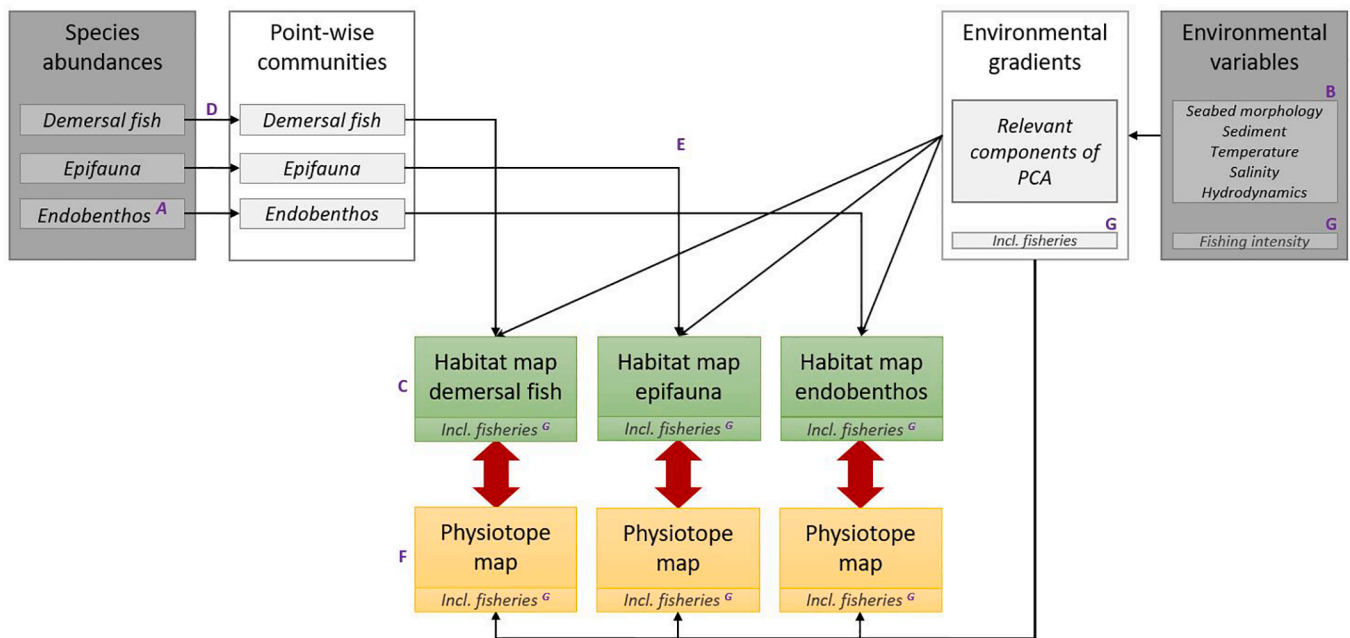


**Fig. 1.** Schematic overview of the methodology presented in this paper to create the final habitat (green boxes) and physiotope (yellow boxes) maps. Grey boxes depict input data. Purple letters refer to appendices where additional information can be found regarding the selection procedure of endobenthos data (A), the environmental variables used (B), the characteristics of resulting habitat maps (C), a comparison in clustering methodology (D), a comparison of interpolation methodology (E), the characteristics of resulting physiotores (F), and the added value of fishing intensity as explanatory variable (G). (For interpretation of the references to colour in this figure legend, the reader is referred to the web version of this article.)

sampled epifauna with a small beam trawl (2 m width, 5 mm mesh size). Five-min hauls were performed at 1 knot (covering  $\sim 300 \text{ m}^2$ ) at 283 stations (Fig. 3B). All caught organisms were determined to the lowest possible taxonomic level (see detailed methodology in Callaway et al., 2002). A checked and cleaned version of the dataset was used here, comprising a list of species abundances (in total number or weight per  $\text{m}^2$ , depending on the species) per station (Robinson, Unpublished data). We removed stations outside our study area, species that were not epifauna, species that appeared in  $< 5$  stations, and species without any weight or number recordings. Registrations with some unquantified presences were given the species-specific minimum observed weight/number per  $\text{m}^2$ .

### 2.2.3. Endobenthos

For infauna, we used the data sampled with a boxcore or grab (covering  $\sim 0.071 \text{ m}^2$ ) in the internationally harmonized North Sea Benthos Survey (NSBS) in 1986 (Kunitzer et al., 1992). The stations were regularly distributed across the entire North Sea (Fig. 3C). Samples were sieved over a 1 mm sieve and all organisms were subsequently identified to the lowest level possible, resulting in a dataset of species densities (see Heip et al., 1992 for detailed methodology). This dataset was obtained from the EMODnet Biology data portal (EMODnet Biology, 2018). Subsequent endobenthos surveys have been performed since the NSBS, but these could unfortunately not be merged in a single, sufficiently uniform dataset (results shown in Appendix A). To increase replicability of our study, we decided to only use the well-tested NSBS dataset, despite its age. Sampling stations outside our study area were removed, as were species that appeared in  $< 5$  stations, and species without any recorded densities.

### 2.3. Biological clustering

Each biological dataset was analysed separately. We determined Bray-Curtis dissimilarities in community composition between sampling stations based on the fourth root of species densities (Reiss et al., 2010). Hierarchical clustering was then done using an average linkage sorting

(Oksanen et al., 2019; Reiss et al., 2010), adopting a Flexible Dissimilarity Height (FDH-) approach. Based on visual inspection of the dendrograms, we performed a first cut-off at 0.50. Stations that were then in clusters with  $\leq 5$  stations were subsequently merged with larger clusters, as long as the dissimilarity height did not exceed 0.60. Remaining clusters with  $\leq 5$  stations were then removed as outliers. In Appendix D, we test the robustness of this approach by comparing it to a Fixed Number (FN-) approach, which identified a fixed number of clusters (here: 5, 10, 15) without considering dissimilarity height or cluster size.

### 2.4. Physiotores

A total of 21 environmental variables were included in the physiotope clustering (Table 1; see Appendix B for detailed descriptions and figures of each individual variable). We additionally investigated the added value of fishing intensity as an explanatory, anthropogenic variable, which is further described in Appendix G.

All environmental variables were bilinearly interpolated to the highest resolution available ( $\sim 180 \times 180 \text{ m}$ ). Physiotope classification followed the methodology described in (Verfaillie et al., 2009). To avoid collinearity, all variables were summarized with a Principal Component Analysis (PCA) into environmental gradients. The first seven principal components (eigenvalue  $> 1$ ) were kept, which together explained 77.5% of the observed variation. A hierarchical cluster analysis was performed on all grid cells, based on these seven main environmental gradients, using Wards method in the 'Rclusterpp' package (Linderman, 2013). Subsequent K-means partitioning used the hierarchical tree as starting points and were set to yield equal numbers of clusters as defined for biological assemblages, to facilitate the comparison between physiotores and habitat maps.

### 2.5. Modelling habitat distributions

Habitat distributions were determined by applying Random Forest machine learning algorithm to the identified biological assemblages for the three faunal groups separately (Breiman, 2001). The Random Forest

**Table 1**  
Environmental variables used in this study, and the anthropogenic variable fishing intensity as used in appendix G.

| Environmental variable  | Explanation                                                                                                                                                            | Source                                                                                                                    |
|-------------------------|------------------------------------------------------------------------------------------------------------------------------------------------------------------------|---------------------------------------------------------------------------------------------------------------------------|
| Depth                   | Absolute water depth                                                                                                                                                   | (EMODnet, 2019a)                                                                                                          |
| BPI-5                   | Depth relative to its surrounding, using a 5 km-radius                                                                                                                 | Derived from the bathymetry data                                                                                          |
| BPI-50                  | Depth relative to its surrounding, using a 50 km-radius                                                                                                                | Derived from the bathymetry data                                                                                          |
| BPI-500                 | Depth relative to its surrounding, using a 500 km-radius                                                                                                               | Derived from the bathymetry data                                                                                          |
| Slope                   | Angle of the seabed compared to a flat seabed                                                                                                                          | Derived from the bathymetry data                                                                                          |
| Northness               | Cosine of the compass direction of the seabed slope                                                                                                                    | Derived from the bathymetry data                                                                                          |
| Eastness                | Sine of the compass direction of the seabed slope                                                                                                                      | Derived from the bathymetry data                                                                                          |
| Mean temperature        | Average of the monthly temperature at the seabed over 2008–2017                                                                                                        | Atlantic-European North West Shelf – Ocean Physics Analysis and Forecast Model by MetOffice (Copernicus, 2019)            |
| Maximum temperature     | Average of the annual maximum monthly temperature at the seabed over 2008–2017                                                                                         | Derived from the temperature data                                                                                         |
| Minimum temperature     | Average of the annual minimum monthly temperature at the seabed over 2008–2017                                                                                         | Derived from the temperature data                                                                                         |
| Temperature variability | Average of the annual differences in maximum and minimum monthly temperatures at the seabed over 2008–2017                                                             | Derived from the temperature data                                                                                         |
| Mean salinity           | Average of the monthly salinity at the seabed over 2008–2017                                                                                                           | Atlantic-European North West Shelf – Ocean Physics Analysis and Forecast Model by MetOffice (Copernicus, 2019)            |
| Salinity variability    | Average of the annual differences in maximum and minimum monthly salinity at the seabed over 2008–2017                                                                 | Derived from the salinity data                                                                                            |
| Mean mixed layer depth  | Average of the annual monthly mixed layer depth over 2008–2017                                                                                                         | Atlantic-European North West Shelf – Ocean Physics Analysis and Forecast Model by MetOffice (Copernicus, 2019)            |
| Mixtures                | Average number of months per year that the water column is completely mixed                                                                                            | Derived from the bathymetry and mixed layer depth data                                                                    |
| Average wind-driven BSS | Annual average of daily wind-driven bed shear stress, determined from modelled wave height and peak period values combined with bathymetry data over 2015–2017         | Atlantic-European North West Shelf – Ocean Wave Analysis and Forecast Model by MetOffice (Copernicus, 2019)               |
| Maximum wind-driven BSS | Average of annual maximum daily wind-driven bed shear stress, determined from modelled wave height and peak period values combined with bathymetry data over 2015–2017 | Derived from the wave and bathymetry data                                                                                 |
| Tidal-driven BSS        | Modelled estimates of tidal bed shear stress                                                                                                                           | Obtained from a hydrodynamic model by John Aldridge (CEFAS), as used in (Hiddink et al., 2006; van Denderen et al., 2015) |
| Mud                     | The modelled fraction of mud                                                                                                                                           | (Stephens and Diesing, 2015; Stephens, 2015)                                                                              |

**Table 1 (continued)**

| Environmental variable        | Explanation                                                       | Source                                       |
|-------------------------------|-------------------------------------------------------------------|----------------------------------------------|
| Sand                          | The modelled fraction of sand                                     | (Stephens and Diesing, 2015; Stephens, 2015) |
| Gravel                        | The modelled fraction of gravel                                   | (Stephens and Diesing, 2015; Stephens, 2015) |
| <b>Anthropogenic variable</b> |                                                                   |                                              |
| Fishing intensity*            | The average annual international fishing intensity over 2010–2012 | (Eigaard et al., 2017)                       |

\* The usage of this variable as an explanatory variable is further described in Appendix G.

classifier calculated the probability for a grid cell to belong to each assemblage, based on the main environmental gradients. This avoided collinearity of individual environmental variables and provided equal weight to the different gradients. Each model encompassed 500 internal runs. This resulted in three habitat maps with a resolution of  $\sim 180 \times 180$  m. Model accuracy was interpreted from ‘Out-of-Bag’ (OOB)-estimates and the median kappa value obtained from a cross-validation based on 100 iterations with half of the input data, using the ‘rUtilities’ package (Evans and Murphy, 2018). We also determined spatial accuracy patterns. For this, a cross-validation was performed on five cluster-stratified folds after which the Shannon diversity index was determined for each grid cell. This index is 0 when grid cells were assigned to the same habitat (cluster) in all 5 predicted maps (so high accuracy), and increases to 1.6 when the cell was assigned to a different cluster in all 5 maps. The more different habitats a cell was assigned to in the 5 maps, and the more equal the proportional abundances of the five habitats were in the 5 runs, the more difficult it is to correctly predict which habitat the cell would be assigned to the next run. The Shannon entropy therefore quantifies the uncertainty (entropy or degree of surprise) associated with this prediction.

In Appendix E, the added value of environmental knowledge in the interpolation step is investigated. For this, we created alternative full-coverage habitat maps, using the Nearest Neighbour method (NN-approach). This method applies *Voronoi* tessellation (Hijmans et al., 2017; Turner, 2019) on the point-wise biological clusters.

### 2.5.1. Anthropogenic pressures

We studied habitat associations of anthropogenic pressures by comparing the spatial distributions of habitats and anthropogenic activities. As anthropogenic variables we used international demersal fishing intensity, given as the average annual swept area ratio (SAR;  $\text{year}^{-1}$ ) over 2010–2012 (Eigaard et al., 2017), and rasterized shapefiles of OWFs (EMODnet, 2019b) and Natura-2000 areas (EEA, 2018). Grid cells with a SAR > 1 were classified as ‘fished’, and average fishing intensity of the fished cells was calculated. In addition, habitat-specific extents were determined for the presence of OWFs and Natura-2000 areas. Finally, we compared fishing pressure and OWF presence in and outside of Natura-2000 areas.

## 3. Results

### 3.1. Habitat maps

The datasets used for demersal fish, epifauna, and endobenthos included 1501, 192, and 149 stations and 73, 147, and 200 species, respectively. Hierarchical clustering resulted in 6, 13, and 10 assemblages for demersal fish, epifauna, and endobenthos, respectively, that were interpolated to full-scale habitat maps (Fig. 4; Table 2; see Appendix C for detailed descriptions of the habitats and their characteristic species and environmental conditions). Herein, the FDH-approach was favoured over the FN-approach to determine the assemblages because it corrected for deviating stations that were unique clusters in the FN-

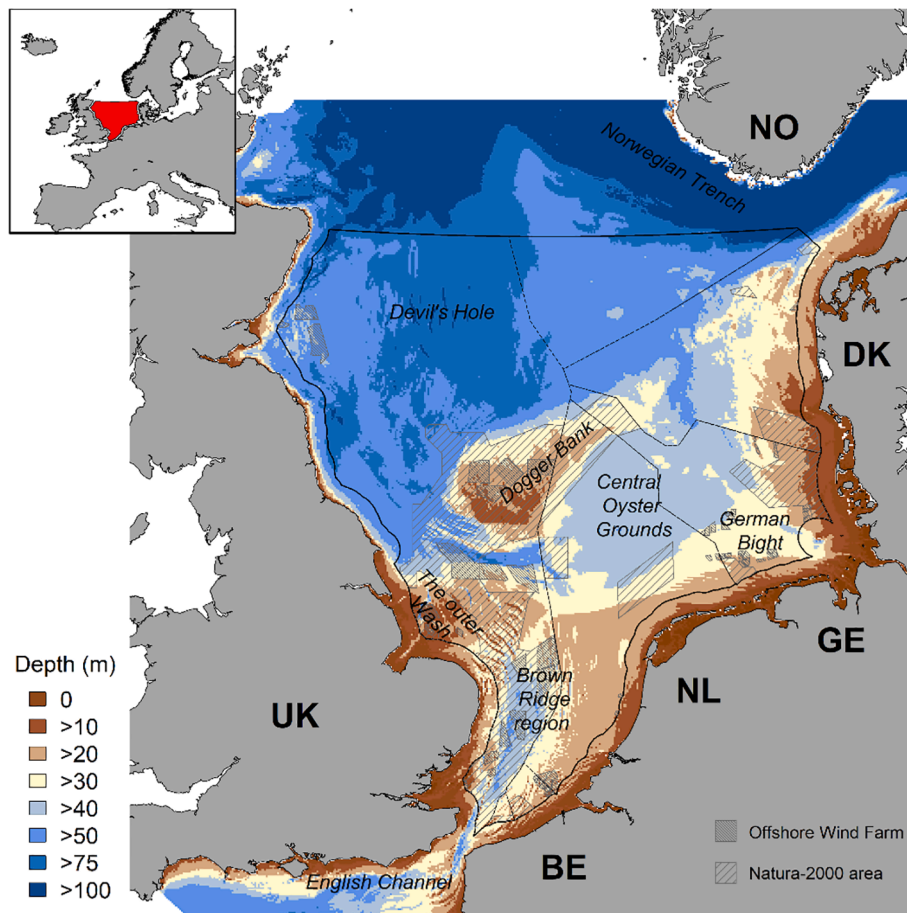


Fig. 2. Bathymetry of the southern North Sea, including names of important subareas. The study area is delineated with a black solid line. Grey hatched areas depict Natura-2000 areas and offshore wind farms, and two-letter codes reflect surrounding countries. Black dotted lines represent Exclusive Economic Zones (EEZ).

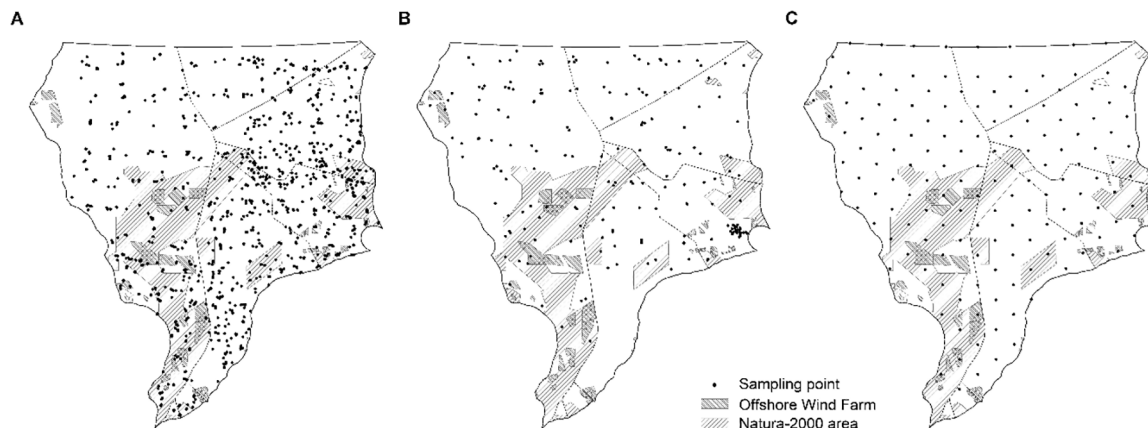
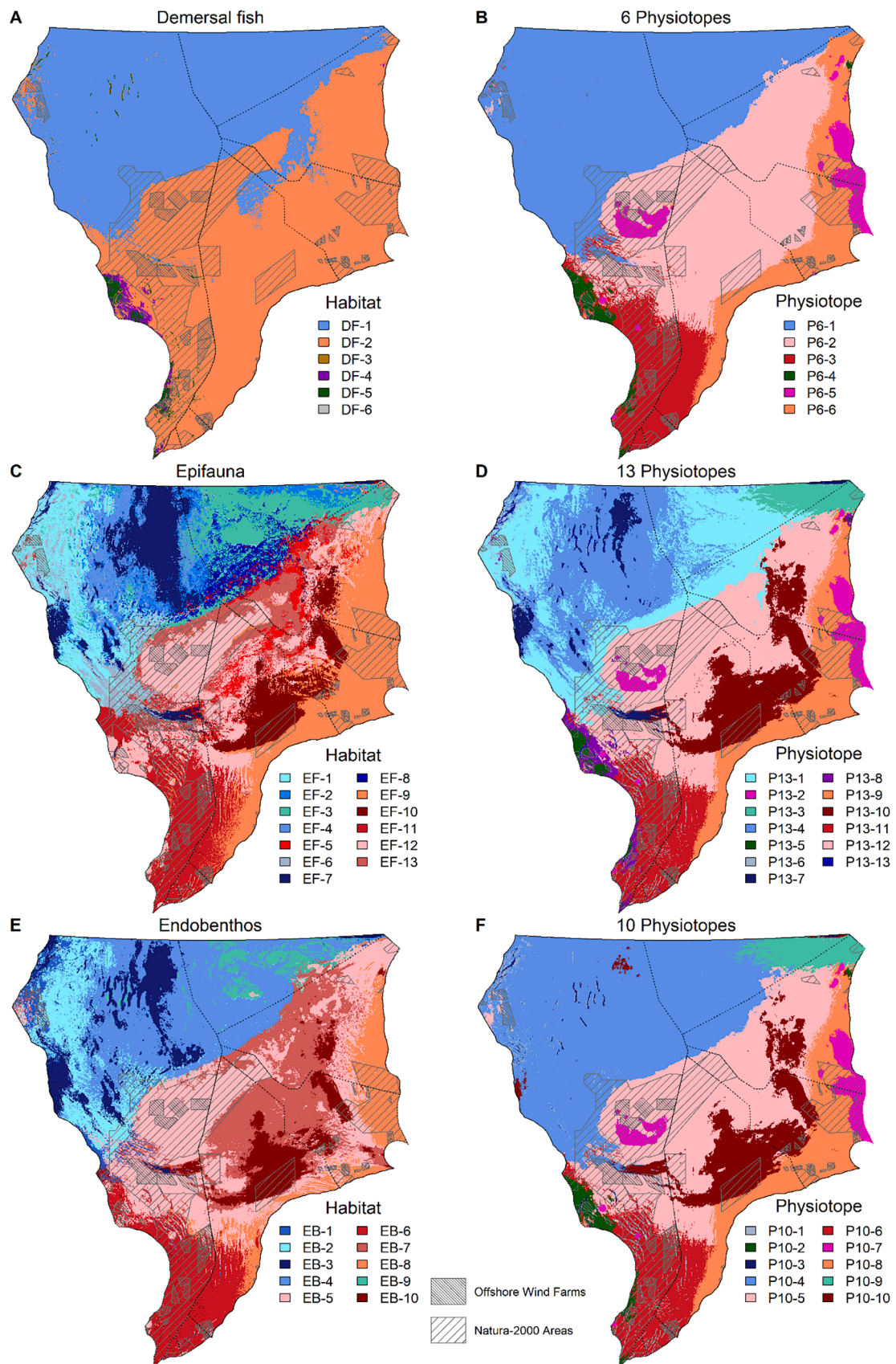


Fig. 3. Sampling locations for demersal fish (A), epifauna (B), and endobenthos (C) within the study areas. Grey hatched areas depict Natura-2000 areas and offshore wind farms. Black dotted lines represent Exclusive Economic Zones (EEZ).

approach (Appendix D). Secondly, the Random Forest models were favoured over the NN-approach (Appendix E) as their results matched better with our independent knowledge of the heterogeneity of the North Sea. Moreover, fishing intensity was not included as an explanatory variable as it did not alter the habitat distributions (Appendix G).

The spatial extent of different habitat varied between faunal groups (DF: 0–53%; EF: 3–16%; EB: 3–23%; Table 2). However, general patterns could be observed among the three faunal groups (Fig. 4). Although the deeper waters northwest of the Dogger Bank were typified

as one large demersal fish habitat (DF-1), they contained multiple epifauna and endobenthos habitats. These were located near the Norwegian trench (EF-2&3, EB-9), the Devil's Hole (EF-7, EB-3), the western coast (EF-1, EB-1&2) and the central North Sea (EF-4&8, EB-4) (Fig. 4). The shallower waters southeast of the Dogger Bank showed a similar pattern. Habitat DF-2 for demersal fish covered the entire area, whereas distinct epifauna and endobenthos habitats separated between the Brown Bank region (EF-11, EB-6), the Central Oyster Grounds (EF-10, EB-10), around the Dogger Bank (EF-5, 12&13, EB-5 & 7), and the



**Fig. 4.** The spatial distribution of demersal fish (A), epifauna (C), and endobenthos (E) habitats, and the corresponding maps with comparable numbers of physiopes (B:6, D:13, F:10). Grey hatched areas depict Natura-2000 areas and offshore wind farms. Black dotted lines represent national economic exclusive zones.

**Table 2**  
Model accuracy\*, habitat details\*\*, and anthropogenic pressures\*\*\* for demersal fish, epifauna, and endobenthos habitat maps.

| Habitat            | Model accuracy details |              | Habitat details |             | Anthropogenic usage |                  |              |                                    |          |                               |                      |                    |                              |                           |       |
|--------------------|------------------------|--------------|-----------------|-------------|---------------------|------------------|--------------|------------------------------------|----------|-------------------------------|----------------------|--------------------|------------------------------|---------------------------|-------|
|                    | Nr. Stations           | Class. Error | User acc        | Pred acc    | Overall Kappa       | OOB-estimate (%) | Coverage (%) | Extent (x 10,000 km <sup>2</sup> ) | % Fished | Fishing intensity (mean ± SD) | % Offshore wind farm | % Natura-2000 area | % Fished in Natura-2000 area | % OWF in Natura-2000 area |       |
| Demersal fish      | DF-1                   | 402          | 0.080           | 92.2        | 93.2                | 0.824            | 8.36         | 44.87                              | 12.67    | 32.13                         | 4.36 ± 3.87          | 0.66               | 3.69                         | 42.66                     | 0.08  |
|                    | DF-2                   | 1007         | 0.041           | 96.1        | 92.9                |                  |              | 53.48                              | 15.10    | 48.07                         | 3.20 ± 2.83          | 5.86               | 36.85                        | 43.96                     | 10.64 |
|                    | DF-3                   | 28           | 1.000           | 0.0         | 0.0                 |                  |              | 0.01                               | 0.00     | 61.15                         | 2.62 ± 1.30          | 0.42               | 23.14                        | 19.27                     | 1.83  |
|                    | DF-4                   | 21           | 0.238           | 79.4        | 80.7                |                  |              | 0.79                               | 0.22     | 8.79                          | 3.53 ± 3.45          | 11.09              | 41.43                        | 17.32                     | 8.90  |
|                    | DF-5                   | 31           | 0.323           | 70.9        | 74.4                |                  |              | 0.85                               | 0.24     | 27.41                         | 5.42 ± 4.46          | 9.62               | 48.16                        | 26.39                     | 10.08 |
|                    | DF-6                   | 10           | 1.000           | 0.0         | NA                  |                  |              | 0.00                               | 0.00     | 32.62                         | 4.93 ± 3.66          | 1.07               | 100                          | 32.62                     | 1.07  |
| Epifauna           | EF-1                   | 10           | 0.600           | 40.4        | 40.4                | 0.590            | 37.18        | 9.25                               | 2.61     | 29.25                         | 4.14 ± 3.29          | 3.41               | 9.30                         | 35.72                     | 1.87  |
|                    | EF-2                   | 7            | 1.000           | 82.4        | 79.0                |                  |              | 3.26                               | 0.92     | 33.09                         | 4.84 ± 3.90          | 0.00               | 0.31                         | 7.02                      | 0.00  |
|                    | EF-3                   | 11           | 0.182           | 64.5        | 73.7                |                  |              | 8.78                               | 2.48     | 38.28                         | 5.08 ± 4.18          | 0.29               | 1.43                         | 47.59                     | 0.01  |
|                    | EF-4                   | 8            | 0.500           | 40.0        | 44.9                |                  |              | 5.76                               | 1.63     | 14.77                         | 3.43 ± 2.93          | 0.01               | 0.28                         | 21.09                     | 0.00  |
|                    | EF-5                   | 7            | 0.571           | 20.9        | 17.9                |                  |              | 3.14                               | 0.89     | 54.83                         | 2.80 ± 2.42          | 0.45               | 2.84                         | 50.38                     | 6.06  |
|                    | EF-6                   | 9            | 0.667           | 0.0         | NA                  |                  |              | 4.34                               | 1.23     | 25.14                         | 3.81 ± 3.12          | 3.50               | 31.25                        | 26.61                     | 6.37  |
|                    | EF-7                   | 11           | 0.091           | 81.7        | 61.9                |                  |              | 7.66                               | 2.16     | 32.68                         | 6.21 ± 4.84          | 0.23               | 1.17                         | 56.78                     | 0.01  |
|                    | EF-8                   | 6            | 0.333           | 50.1        | 38.9                |                  |              | 3.30                               | 0.93     | 23.72                         | 2.15 ± 1.67          | 0.00               | 0.52                         | 65.24                     | 0.00  |
|                    | EF-9                   | 44           | 0.091           | 42.9        | 59.8                |                  |              | 16.29                              | 4.60     | 45.85                         | 3.63 ± 3.06          | 2.43               | 22.92                        | 30.76                     | 1.36  |
|                    | EF-10                  | 9            | 0.222           | 33.6        | 36.7                |                  |              | 6.25                               | 1.77     | 45.01                         | 2.38 ± 1.96          | 0.81               | 14.52                        | 40.12                     | 1.16  |
|                    | EF-11                  | 9            | 0.444           | 90.6        | 90.3                |                  |              | 11.15                              | 3.15     | 45                            | 3.73 ± 3.12          | 10.94              | 58.56                        | 34.48                     | 14.59 |
|                    | EF-12                  | 15           | 0.533           | 77.0        | 56.9                |                  |              | 14.29                              | 4.03     | 53.07                         | 3.00 ± 2.75          | 8.05               | 46.62                        | 61.99                     | 13.45 |
|                    | EF-13                  | 10           | 0.800           | 92.0        | 90.5                |                  |              | 6.54                               | 1.85     | 52.83                         | 2.53 ± 2.39          | 3.89               | 26.12                        | 47.02                     | 8.86  |
| Endobenthos        | EB-1                   | 6            | 1.000           | 11.2        | 20.0                | 0.580            | 35.29        | 2.82                               | 0.80     | 30.12                         | 4.21 ± 3.52          | 8.64               | 14.16                        | 31.43                     | 2.16  |
|                    | EB-2                   | 9            | 0.556           | 91.9        | 75.5                |                  |              | 7.75                               | 2.19     | 29.69                         | 4.12 ± 3.16          | 1.58               | 10.99                        | 33.14                     | 0.00  |
|                    | EB-3                   | 8            | 0.375           | 48.5        | 47.6                |                  |              | 5.90                               | 1.67     | 38.67                         | 6.70 ± 4.93          | 0.00               | 1.25                         | 54.92                     | 0.00  |
|                    | EB-4                   | 21           | 0.048           | 56.4        | 67.5                |                  |              | 19.53                              | 5.51     | 19.11                         | 3.11 ± 2.81          | 0.01               | 1.06                         | 34.12                     | 0.00  |
|                    | EB-5                   | 22           | 0.409           | 90.9        | 67.7                |                  |              | 22.74                              | 6.42     | 47.88                         | 3.42 ± 3.18          | 8.31               | 46.61                        | 50.01                     | 12.56 |
|                    | EB-6                   | 8            | 0.250           | 55.8        | 56.4                |                  |              | 9.10                               | 2.57     | 54.47                         | 3.80 ± 3.12          | 10.36              | 53.88                        | 39.01                     | 15.36 |
|                    | EB-7                   | 22           | 0.273           | 75.0        | 75.6                |                  |              | 15.58                              | 4.40     | 50.45                         | 2.80 ± 2.52          | 0.94               | 8.17                         | 46.65                     | 2.24  |
|                    | EB-8                   | 8            | 0.875           | 70.1        | 68.5                |                  |              | 7.56                               | 2.13     | 46.41                         | 3.93 ± 3.26          | 2.58               | 34.87                        | 28.22                     | 1.33  |
|                    | EB-9                   | 6            | 0.400           | 22.3        | 35.0                |                  |              | 3.36                               | 0.95     | 45.68                         | 5.57 ± 4.2           | 0.00               | 0.70                         | 79.46                     | 0.00  |
|                    | EB-10                  | 10           | 0.100           | 50.6        | 100.0               |                  |              | 5.66                               | 1.60     | 44.51                         | 2.47 ± 2.07          | 0.96               | 20.13                        | 39.18                     | 1.16  |
| Overall study area | 100.00                 | 28.24        | 40.43           | 3.63 ± 3.30 | 3.60                | 22.10            | 43.14        | 9.81                               |          |                               |                      |                    |                              |                           |       |

\* Model accuracy details comprise the number of stations within an identified habitat (Nr. Stations), habitat-specific classification error (Class. Error) of the full model, and user (User acc) and prediction (Pred acc) accuracy estimates for the cross-validations. Overall Kappa and OOB-estimates are shown per model.

\*\* Habitat details comprise the spatial coverage (%) and extent (in km<sup>2</sup>).

\*\*\* Anthropogenic pressures are displayed as the % of area that is fished (intensity > 1 year<sup>-1</sup>), used for offshore wind farms, and designated as Natura-2000 area. Mean (±SD) fishing intensity (year<sup>-1</sup>) is given for the fished (intensity > 1 year<sup>-1</sup>) area. In addition, the habitat-specific percentage of Natura-2000 areas covered by the spatial extent of fishing activity and OWFs is given.

eastern coast (EF-9, EB-8). Interestingly, the two demersal fish habitats identified very locally near the outer Wash (DF-4, DF-5) did not have equivalent distinct epifauna or endobenthos habitats.

The demersal fish Random Forest model had an overall Kappa of 0.82 and an OOB-estimate of 8%, showing a reliable prediction of the habitats (Table 2). Prediction accuracy was lowest for the smallest habitats (<0.01% coverage) DF-3 and DF-6, whereas the slightly larger sized (<1%) habitats DF-4 and DF-5 already showed accuracies of > 74% (Table 2). For epifauna and endobenthos, models showed reasonable, but lower overall Kappa values (0.59 and 0.58 respectively) and higher OOB-estimates (37% and 35% respectively; Table 2). Habitat extent, number of observations within the cluster, and habitat-specific accuracy were not clearly related (Table 2). Spatial patterns in accuracy differed between the three models (Fig. 5.) Uncertainty in demersal fish habitats was dominantly restricted to the Central Oyster Grounds and south of the Dogger Bank (Fig. 5A). For epifauna and endobenthos, higher Shannon diversity values were more common and widespread over the study area, representing lowered model consistency between the five cross-validations. Whereas the classifications of epifauna habitats were most consistent in the eastern and southern North Sea (Fig. 5B), endobenthos habitats were classified more consistently at the Dogger Bank, Central Oyster Grounds and the Brown Ridge Region (Fig. 5C).

### 3.2. Physiotypes

We applied hierarchical and K-means clustering on all grid cells, based on their score on the seven main environmental gradients resulting in high-resolution physiotype maps with 6, 13, and 10 clusters (P6, P10, P13; Fig. 4; see Appendix F for detailed environmental information of the physiotypes). To facilitate the comparison with the habitat maps, we visually matched the naming of individual physiotypes and habitats based on approximately shared locations. All three physiotype maps showed large ranges in spatial extent between physiotypes (P6: 1–41%; P10: 0–37%; P13: 0–23%; Table 3).

All physiotype maps showed a distinction between the deep waters northwest of the Dogger Bank and the shallow waters to its southeast (Fig. 4). The P6-map (Fig. 4B) distinguished 5 physiotypes in the southeast: Brown Bank region (P6-3), eastern coast (P6-6), central North Sea (P6-2), outer Wash (P6-4), and a combination of the shallowest part of the Dogger Bank with a strip along the southern Danish coast (P6-5). These physiotypes largely remain the same in the P10- and P13-maps, although some physiotypes become divided into smaller ones (Fig. 4D&F). A relatively large (9%) physiotype was associated with the Central Oyster Grounds (P10-10, P13-10), while several relatively small

(<5%) physiotypes were identified as well. These comprised the edge of the Norwegian Trench (P10-9, P13-3), sand ridge troughs in the Brown Bank region (P10-1, P13-6), and the deep trenches of Devil's Hole (P10-3, P13-13; Fig. 4; Table 3). The northwest waters remained a singly physiotype when 6 and 10 physiotypes were delineated. Only when 13 physiotypes were defined, this area was divided into multiple physiotypes (P13-1, P13-4, P13-7).

### 3.3. Comparison physiotypes and habitats

All physiotype and habitat maps separated the deep waters northwest from the shallower waters southeast (Fig. 4). When taking the P13-map as the leading physiotype map, physiotypes P13-7, P13-9, P13-10, and P13-11 showed a reasonable match with habitat distributions (Fig. 4). For instance, the Brown Bank region (P13-11) was spatially very comparable to habitats EF-11 and EB-6. Similarly, distinct physiotypes at the Central Oyster Grounds (P13-10) and along the eastern coast (P13-9) were also represented as habitats (EF-10, EB-10 and EF-9, EB-8 respectively).

Despite this overall similarity, the physiotype map showed several discrepancies with the habitat maps. In Fig. 6 we show how much area (in %) of a habitat overlaps with each physiotype, as an addition to visual comparison. When all habitats and physiotypes perfectly match, a strict declining diagonal should emerge, which is not the case (Fig. 6). This is mainly caused by habitats that cover multiple physiotypes or vice versa. The demersal fish habitat DF-2, for instance, comprised almost all physiotypes, except for P6-1 (Fig. 6A). Contrary, the physiotype P10-4 covered endobenthos habitats EB-2, 3, 4, & 9 (Fig. 6C; Fig. 4) and the physiotypes P13-1 and P13-12 were unable to detect environmental differences between epifauna habitats EF-1, 3, 5, 6, & 8 and EF-5, 9, 11, 12 & 13 respectively (Fig. 6B; Fig. 4). Interestingly, all three physiotype maps consistently delineate a physiotype (P6-5, P13-2, P10-7) that covered part of the eastern coast with an additional location at the Dogger Bank (Fig. 4) without an equivalent habitat in any faunal group.

### 3.4. Habitat-specific anthropogenic pressures

All habitats were subjected to demersal fishing and/or offshore wind farms (Table 2). The fished extent (in %) of each habitat varied between 9 and 65 % (Table 2), showing strong associations of demersal fishing with specific habitats. Preferred habitats (>40% fished extent) were dominantly located in the shallow waters southeast. Habitats with large OWF (>5%) and Natura-2000 area (>40%) extents were mostly located in the Brown Bank region and at the Dogger Bank. It should be noted,

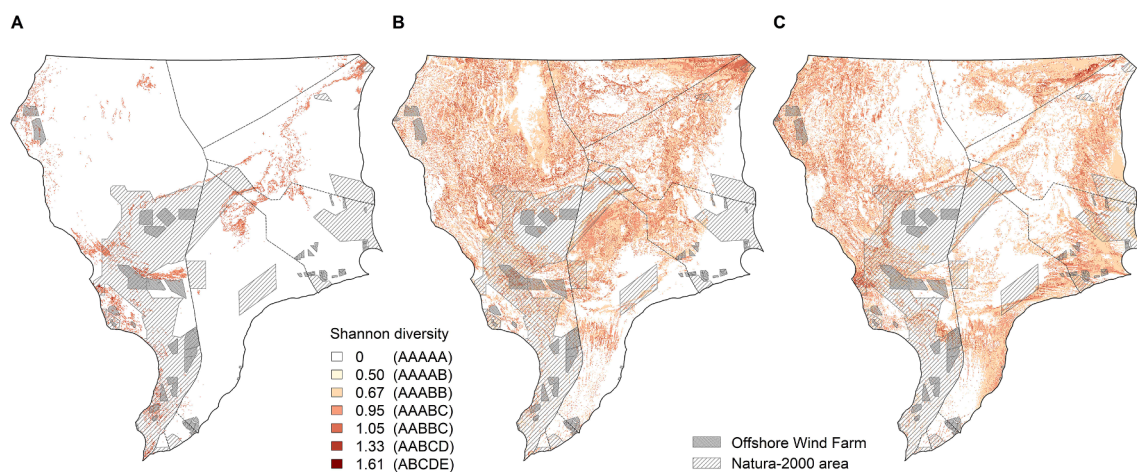
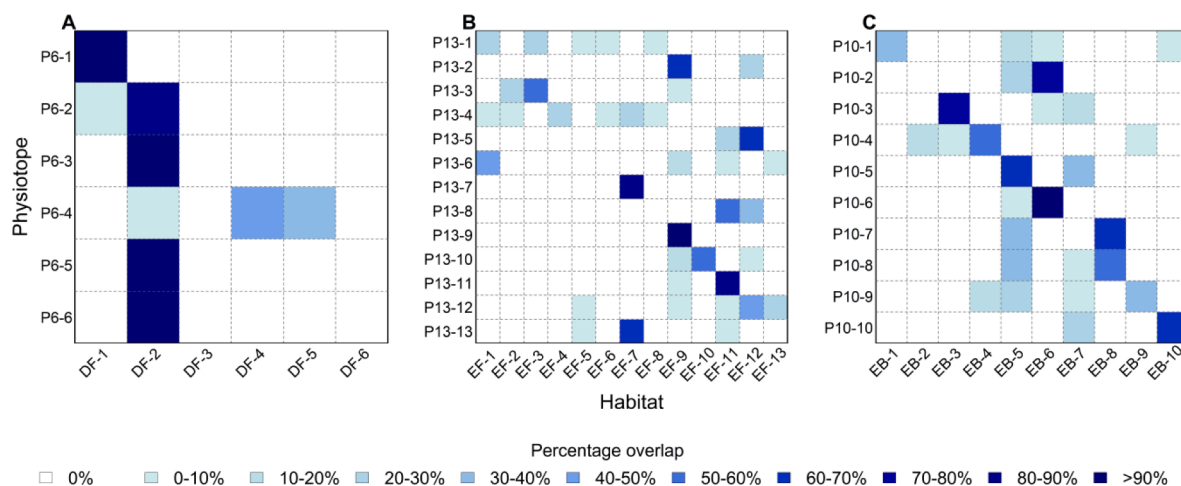


Fig. 5. Spatial accuracy of the Random Forest model for demersal fish (A), epifauna (B), and endobenthos (C). Accuracy is determined as the Shannon diversity index of the model predictions for five cross-validations. Higher values represent a lower consistency of assigned habitats for a grid cell, as indicated with the letters in the legend.

**Table 3**  
Physiotope details as percentage spatial coverage, extent (in km<sup>2</sup>), and anthropogenic pressures\*.

| Physiotope         | Coverage (%) | Extent (x 10.000 km <sup>2</sup> ) | % Fished | Fishing intensity (mean ± SD) | % Offshore wind farm | % Natura-2000 area |       |
|--------------------|--------------|------------------------------------|----------|-------------------------------|----------------------|--------------------|-------|
| 6 Physiotoypes     | P6-1         | 41.25                              | 11.65    | 27.84                         | 4.58 ± 3.97          | 1.07               | 4.77  |
|                    | P6-2         | 32.92                              | 9.29     | 50.32                         | 2.69 ± 2.40          | 4.70               | 27.43 |
|                    | P6-3         | 10.45                              | 2.95     | 50.56                         | 3.77 ± 3.10          | 10.35              | 58.28 |
|                    | P6-4         | 1.25                               | 0.35     | 11.73                         | 3.73 ± 3.28          | 10.51              | 39.09 |
|                    | P6-5         | 3.36                               | 0.95     | 54.91                         | 3.85 ± 3.36          | 4.00               | 71.84 |
|                    | P6-6         | 10.78                              | 3.04     | 47.39                         | 4.26 ± 3.54          | 2.41               | 19.66 |
| 13 Physiotoypes    | P13-1        | 19.94                              | 5.63     | 29.14                         | 3.64 ± 3.09          | 2.36               | 9.87  |
|                    | P13-2        | 2.83                               | 0.80     | 54.02                         | 3.96 ± 3.44          | 1.88               | 70.59 |
|                    | P13-3        | 2.82                               | 0.80     | 78.76                         | 6.88 ± 4.46          | 0.00               | 3.60  |
|                    | P13-4        | 17.91                              | 5.06     | 18.46                         | 3.53 ± 3.16          | 0.00               | 1.44  |
|                    | P13-5        | 0.58                               | 0.16     | 6.96                          | 2.85 ± 2.30          | 11.61              | 30.66 |
|                    | P13-6        | 1.46                               | 0.41     | 36.68                         | 4.42 ± 3.65          | 7.11               | 46.01 |
|                    | P13-7        | 2.56                               | 0.72     | 60.51                         | 7.41 ± 5.01          | 0.22               | 2.49  |
|                    | P13-8        | 1.44                               | 0.41     | 16.05                         | 4.53 ± 4.02          | 8.57               | 47.65 |
|                    | P13-9        | 9.23                               | 2.61     | 44.23                         | 3.89 ± 3.17          | 2.54               | 20.67 |
|                    | P13-10       | 9.64                               | 2.72     | 46.98                         | 2.46 ± 1.94          | 1.26               | 11.65 |
|                    | P13-11       | 8.18                               | 2.31     | 57.43                         | 3.79 ± 3.09          | 11.21              | 57.62 |
|                    | P13-12       | 23.17                              | 6.54     | 50.79                         | 2.69 ± 2.43          | 6.43               | 36.20 |
|                    | P13-13       | 0.24                               | 0.07     | 52.96                         | 7.40 ± 4.62          | 4.09               | 19.81 |
| 10 Physiotoypes    | P10-1        | 1.66                               | 0.47     | 36.22                         | 4.51 ± 3.74          | 7.46               | 43.14 |
|                    | P10-2        | 1.21                               | 0.34     | 11.03                         | 3.72 ± 3.19          | 10.61              | 38.95 |
|                    | P10-3        | 0.41                               | 0.12     | 55.76                         | 6.87 ± 4.59          | 3.05               | 18.56 |
|                    | P10-4        | 37.08                              | 10.47    | 23.76                         | 3.94 ± 3.52          | 1.02               | 4.75  |
|                    | P10-5        | 25.93                              | 7.32     | 50.34                         | 2.76 ± 2.51          | 6.05               | 33.86 |
|                    | P10-6        | 8.73                               | 2.47     | 54.52                         | 3.80 ± 3.12          | 10.97              | 57.98 |
|                    | P10-7        | 3.00                               | 0.85     | 54.25                         | 3.91 ± 3.41          | 2.33               | 70.61 |
|                    | P10-8        | 9.82                               | 2.77     | 44.18                         | 3.83 ± 3.14          | 2.38               | 19.54 |
|                    | P10-9        | 3.15                               | 0.89     | 78.49                         | 6.78 ± 4.44          | 0.03               | 3.33  |
|                    | P10-10       | 9.00                               | 2.54     | 48.91                         | 2.99 ± 2.91          | 1.33               | 12.12 |
| Overall study area | 100.00       | 28.24                              | 40.43    | 3.63 ± 3.30                   | 3.60                 | 22.10              |       |

\* Anthropogenic pressures are displayed as the % of area that is fished (intensity > 1 year<sup>-1</sup>), used for offshore wind farms, and designated as Natura-2000 area. Mean (±SD) fishing intensity (year<sup>-1</sup>) is given for the fished (intensity > 1 year<sup>-1</sup>) area.



**Fig. 6.** Comparisons between physiotoypes and habitats for demersal fish (A), epifauna (B) and endobenthos (C). For each physiotope (Y-axis), the spatial overlap (in % of the physiotope extent) with each biological habitat (X-axis) is displayed.

however, that especially the calculation of fished extent is probably less accurate for smaller habitats.

Strong positive correlations were found (analysis on all DF, EF, and EB habitats > 5%) between the habitat-specific extents of OWFs and fished area, and the spatial extent of Natura-2000 area within that habitat (fished:  $R^2 = 0.464$ ,  $p < 0.001$ ; OWF:  $R^2 = 0.884$ ,  $p < 0.0001$ ; Table 2). This analysis, however, does not determine the spatial overlap of the different activities within a habitat. When habitat-specific extents of fisheries and OWFs were determined within Natura-2000 areas, a more nuanced pattern is observed (Table 2), especially when small habitats (<5%) and habitats with little Natura-2000 area (<5%) were excluded. For demersal fisheries, the overall fished extent (40%) did not

differ much from within Natura-2000 sites (43%; Table 2). However, a larger fished extent inside Natura-2000 areas was observed in Dogger Bank habitat EF-12 (61% compared to 52%), while smaller extents were shown for habitats in the Brown Bank region (EF-11: 35% versus 45%; and EB-6: 39% versus 54%; Table 2) and near the Danish coast (EF-9: 30% versus 46%; and EB-8: 28% versus 46%; Table 2). OWFs, on the other hand, were generally three times larger within Natura-2000 areas (9%) compared to the overall study area (3%; Table 2). Especially in the habitats EF-12 and EB-5, which are located at the Dogger Bank, and habitats EF-11 and EB-6 which cover the Brown Bank region, large parts (>10%) of OWFs were constructed within Natura-2000 areas (Table 2).

#### 4. Discussion

Creating accurate, high-resolution marine habitat maps is challenging (ICES, 2019a), but essential for ecology-inclusive marine spatial planning (White et al., 2012). Here, we developed a novel method that combines point-wise biological data with grid-based environmental variables to create full coverage, high resolution habitat maps. We expand earlier work in the spatial modelling of species assemblages (see e.g. Ferrier & Guisan, 2006; Rubidge, Gale, & Curtis, 2016; Smoliński et al., 2017) by (i) the modelling of both physiotopes and observed assemblages for different faunal groups, (ii) our explorations in the usage of environmental gradients based on environmental and anthropogenic variables (Appendix G), and (iii) the direct comparison between habitat types and anthropogenic activities. As a result, our final habitat maps represent benthic assemblage distributions, congruent to spatial patterns in benthic assemblages as previously described by station-based studies (Kröncke et al., 2011; Reiss et al., 2010). Although several habitats showed close resemblance to physiotopes delineated from environmental variables, some essential differences were observed. Several physiotopes did not distinguish between multiple identified habitats, and one physiotope had no equivalent habitat, suggesting that important environmental variables or ecological processes might not have been captured in the delineation of physiotopes and habitats. Furthermore, we showed that separating maps for three faunal groups – demersal fish, epifauna, and endobenthos – yielded substantially different habitat maps, as expected based on their differences in ecology and mobility. By spatially comparing the habitats identified herein with anthropogenic pressures such as demersal fishing and OWFs, we confirmed that these activities have spatial associations with specific habitats (Grothe and Schnieders, 2011; van der Reijden et al., 2018). Hence, to sustainably manage anthropogenic pressures, habitat-specific impact assessments should be undertaken for the main faunal groups of benthic assemblages. Our findings provide an important new approach to marine habitat mapping, which will enable improvement of habitat-specific impact assessments for ecology-inclusive marine spatial planning.

The presented methodology enabled the inclusion of distinct environmental variables which were relevant to specific communities and faunal groups (Hewitt et al., 2015; Lecours et al., 2015) and avoided subjective choices regarding included variables and exact classification boundaries. As a consequence, the resulting habitat maps predicted a substantially different spatial distribution of benthic assemblages compared to physiotopes maps, including the ones currently used for marine management and spatial planning (Ferrari et al., 2018; ICES, 2020; Rubidge et al., 2016). The Broad Habitat Types under the Marine Strategy Framework Directive (MSFD) are an example of such a currently used habitat map for management of the North Sea. The MSFD aims to achieve Good Environmental Status (GES) in all marine EU waters, for instance by the conservation of seafloor integrity (European Commission, 2008). Seafloor integrity is assessed by habitat-specific analyses of fishing pressures and sensitivity (ICES, 2019b; 2020). This assessment uses the MSFD Broad Habitat Types (MSFD-BHT<sup>1</sup>), which are dominantly based on water depth and sediment type (EMODnet, 2018; ICES, 2020). However, these MSFD-BHT show different habitat distributions compared to our maps, with higher habitat complexity than the demersal fish level, but lower complexity for both epifauna and endobenthos. Most remarkably, the clear distinction between the deeper northwest and shallower waters southeast of the Dogger Bank, which was dominant in all three presented habitat maps, is not captured by the MSFD-BHT map. Some resulting discrepancies between expected benthic assemblages and MSFD-BHT were already recognized during the assessment (ICES, 2019b), and more of such mismatches are likely given our results. These mismatches probably affect the required estimate of

habitat sensitivity, which is parameterized by both habitat- and gear-specific depletion and recovery rates after a bottom trawl pass (Hidink et al., 2017; 2019;; Rijnsdorp et al., 2018). Especially habitat-specific recovery rates, based on longevity estimates of local endobenthos abundances will probably change if the boundaries of endobenthos habitats are adjusted (ICES, 2020; Rijnsdorp et al., 2018). In addition, a similar or integrated analysis for epifauna and demersal fish assemblages would allow for an assessment of the overall demersal ecosystem. Hence, our case-study showed that the current assessments of fishing impact on seafloor integrity probably fail to capture the true ecological status of benthic and demersal assemblages. Similar discrepancies between benthic assemblages and physiotopes have been observed in other areas than the North Sea as well (Ferrari et al., 2018; Rubidge et al., 2016).

Our methodology relies on the interpolation of biological assemblages with environmental variables, and its reliability is thus related to the quality of input data and the ability to apply a correct interpolation. Our input data, especially the endobenthos dataset, showed a spatio-temporal mismatch with the environmental data, increasing the uncertainty of the habitat maps (ICES, 2019a). Environmental data is often surveyed at or modelled to higher spatial and temporal resolution than what is available for biological data, which are generally snapshots in time. This can result in temporal mismatches, both in actual timing and represented time period. As a consequence, the correlations between benthic clusters and environmental gradients used for the interpolation have lower certainty. This can be observed in Fig. 5A, where the demersal fish Random Forest model shows high consistency between all cross-validations, probably because the input data has no spatiotemporal mismatch. The presented endobenthos habitat map has much lower certainty, caused by a large spatiotemporal mismatch in the input data in combination with (anthropogenic) changes in the North Sea since the initial sampling. Recent efforts to merge available endobenthos data for EMODnet demonstrated that the NSBS86 survey is still the leading survey in several regions of the North Sea (P.M.J. Herman, pers. comm.), with limited sampling stations in the northern part of our study area (Rees et al., 2007). And although a comparison of endobenthos composition in 1986 and 2000 showed relatively little difference in the large-scale community distributions (Kröncke et al., 2011), we strongly recommend for a new North Sea Benthos Survey that is internationally harmonized and covers the entire North Sea. Nevertheless, data availability will always dictate what can be used as input data, and therefore spatiotemporal problems will remain. International harmonization of national sampling surveys is therefore required to reduce spatiotemporal mismatches in marine habitat mapping (Appendix A).

#### 5. Conclusions

We demonstrate a new approach to derive high-resolution, full-coverage habitat maps representing benthic assemblages for different faunal groups. The detailed spatial information on benthic assemblages captured by our habitat maps are a first step to true ecology-inclusive marine spatial planning (Ferrari et al., 2018; Kaiser et al., 2016; Rubidge et al., 2016; White et al., 2012). Nonetheless, we find that the quality of the input data is key for accurate output, which demands international harmonization of existing sampling surveys. Our detailed overview in spatial distribution of both habitats and anthropogenic pressures identifies potential areas of conflicting interests and facilitate discussions on a fair balance between economic and ecological values. Assembly-specific knowledge based on species traits and species-environment feedbacks, leading to assessments of resilience, sensitivity, and longevity, can now further improve habitat-specific impact assessments and subsequent management.

#### CRedit authorship contribution statement

**Karin J. Reijden:** Conceptualization, Methodology, Validation,

<sup>1</sup> See: <https://www.emodnet-seabedhabitats.eu/access-data/launch-map-viewer/>

Formal analysis, Data curation, Writing - original draft, Visualization. **Laura L. Govers:** Conceptualization, Methodology, Writing - review & editing, Supervision. **Leo Koop:** Methodology, Writing - review & editing. **Johan H. Damveld:** Methodology, Resources. **Peter M.J. Herman:** Methodology, Resources, Writing - review & editing. **Sebastian Mestdagh:** Writing - review & editing. **Gerjan Piet:** Resources, Writing - review & editing. **Adriaan D. Rijnsdorp:** Writing - review & editing. **Grete E. Dinesen:** Writing - review & editing. **Mirjam Snellen:** Supervision, Project administration, Funding acquisition, Writing - review & editing. **Han Olff:** Conceptualization, Methodology, Project administration, Funding acquisition, Writing - review & editing.

## Declaration of Competing Interest

The authors declare that they have no known competing financial interests or personal relationships that could have appeared to influence the work reported in this paper.

## Acknowledgements

We would like to thank the Centre for Information Technology of the University of Groningen for their support and for providing access to the Peregrine high-performance computing cluster. We also thank Raphaël Scherrer for his assistance with MatLab calculations, Olivier Beauchard for his help in the compilation of the endobenthos dataset, and Alireza Amiri-Simkooei for his valuable comments on earlier versions of the manuscript. This work was funded by the Gieskes-Strijbis Fonds, The Netherlands. LG was funded by NWO grant 016.Veni.181.087. The funders had no involvement in the execution of the study.

### Data availability.

Environmental data used, and resulting spatial maps of biological habitats and physiotoxes are made available as geoTIFFS at the University of Groningen Dataverse repository: <https://doi.org/10.34894/POBLBF>, as well as at an interactive online webmap: [shorturl.at/iqEQ3](http://shorturl.at/iqEQ3).

## Appendix A. Supplementary data

Supplementary data to this article can be found online at <https://doi.org/10.1016/j.ecolind.2021.107849>.

## References

- Andersen, J.H., Manca, E., Agnesi, S., Al-Hamdani, Z., Lillis, H., Mo, G., Populus, J., Reker, J., Tunesi, L., Vasquez, M., 2018. European broad-scale seabed habitat maps support implementation of ecosystem-based management. *Open J. Ecol.* 08 (02), 86–103. <https://doi.org/10.4236/oje.2018.82007>.
- Beisiegel, K., Darr, A., Gogina, M., Zettler, M.L., 2017. Benefits and shortcomings of non-destructive benthic imagery for monitoring hard-bottom habitats. *Mar. Pollut. Bull.* 121 (1–2), 5–15. <https://doi.org/10.1016/j.marpolbul.2017.04.009>.
- Breiman, L., 2001. Random forests. *Mach. Learn.* 45, 5–32. [https://doi.org/10.1007/978-3-662-56776-0\\_10](https://doi.org/10.1007/978-3-662-56776-0_10).
- Callaway, R., Alsava, J., de Boois, I., Cotter, J., Ford, A., Hinz, H., Jennings, S., Kro, I., Lancaster, J., Piet, G.J., Prince, P., Ehrlich, S., 2002. Diversity and community structure of epibenthic invertebrates and fish in the North Sea. *ICES J. Mar. Sci.* 59, 1199–1214. <https://doi.org/10.1006/jmsc.2002.1288>.
- Compton, T.J., Holthuijsen, S., Koolhaas, A., Dekinga, A., ten Horn, J., Smith, J., Galama, Y., Brugge, M., van der Wal, D., van der Meer, J., van der Veer, H.W., Piersma, T., 2013. Distinctly variable mudscapes: Distribution gradients of intertidal macrofauna across the Dutch Wadden Sea. *J. Sea Res.* 82, 103–116. <https://doi.org/10.1016/j.seares.2013.02.002>.
- Cooper, K.M., Bolam, S.G., Downie, A.-L., Barry, J., 2019. Biological-based habitat classification approaches promote cost-efficient monitoring: An example using seabed assemblages. *J. Appl. Ecol.* 56 (5), 1085–1098. <https://doi.org/10.1111/1365-2664.13381>.
- Copernicus, 2019. Marine Copernicus. <http://marine.copernicus.eu/>.
- Costello, M.J., Ballantine, B., 2015. Biodiversity conservation should focus on no-take Marine Reserves: 94% of marine protected areas allow fishing. *Trends Ecol. Evol.* 30 (9), 507–509. <https://doi.org/10.1016/j.tree.2015.06.011>.
- Damveld, J.H., van der Reijden, K.J., Cheng, C., Koop, L., Haaksmma, L.R., Walsh, C.A.J., Soetaert, K., Borsje, B.W., Govers, L.L., Roos, P.C., Olff, H., Hulscher, S.J.M.H., 2018. Video transects reveal that tidal sand waves affect the spatial distribution of benthic organisms and sand ripples. *Geophys. Res. Lett.* 45 (21), 11,837–11,846. <https://doi.org/10.1029/2018GL079858>.
- de Boer, W.P., Roos, P.C., Hulscher, S.J.M.H., Stolk, A., 2011. Impact of mega-scale sand extraction on tidal dynamics in semi-enclosed basins. An idealized model study with application to the southern North Sea. *Coast. Eng.* 58 (8), 678–689. <https://doi.org/10.1016/j.coastaleng.2011.03.005>.
- EEA, 2018. EEA [WWW Document]. URL <https://www.eea.europa.eu/data-and-maps/data/natura-10#tab-gis-data>.
- Eigaard, O.R., Bastardie, F., Hintzen, N.T., Buhl-Mortensen, L., Buhl-Mortensen, P., Catarino, R., Dinesen, G.E., Fock, H., Geitner, K., Gerritsen, H., Gonzalez, M.M., Jonsson, P., Kavadas, S., Laffargue, P., Lundy, M., Mirelis, G.G., Nielsen, J.R., Papadopoulou, N., Posen, P., Pulcinella, J., Russo, T., Sala, A., Silva, C., Smith, C., Vanelslander, B., Zengin, M., Rijnsdorp, A.D., 2017. The footprint of bottom trawling in European waters: distribution, intensity and seabed integrity. *ICES J. Mar. Sci.* 74, 847–865. <https://doi.org/10.1093/icesjms/fsw194>.
- EMODnet Biology, Q., 2018. European Marine Observation Data Network Biology project, funded by the European Commission's Directorate - General for Maritime Affairs and Fisheries (DG Mare). [WWW Document]. URL [www.emodnet-biology.eu](http://www.emodnet-biology.eu).
- EMODnet, 2018. EUSeaMap: A broad-scale seabed habitat map for European Seas. EMODnet, 2019a. EMODnet Bathymetry [WWW Document]. URL [www.emodnet.eu/bathymetry](http://www.emodnet.eu/bathymetry).
- EMODnet, 2019b. EMODnet HumanActivities [WWW Document]. URL <https://www.emodnet-humanactivities.eu/>.
- European Commission, 2008. Directive 2008/56/EC of the European Parliament and of the Council of 17 June 2008 establishing a framework for community action in the field of marine environmental policy (Marine Strategy Framework Directive), Official Journal of the European Union.
- Evans, J.S., Murphy, M.A., 2018. rUtilities. R package 2.1-3. <https://CRAN.R-project.org/package=rUtilities>.
- Ferrari, R., Malcolm, H., Neilson, J., Lucieer, V., Jordan, A., Ingleton, T., Figueira, W., Johnstone, N., Hill, N., 2018. Integrating distribution models and habitat classification maps into marine protected area planning. *Estuar. Coast. Shelf Sci.* 212, 40–50. <https://doi.org/10.1016/j.ecss.2018.06.015>.
- Ferrier, S., Guisan, A., 2006. Spatial modelling of biodiversity at the community level. *J. Appl. Ecol.* 43 (3), 393–404. <https://doi.org/10.1111/j.1365-2664.2006.01149.x>.
- Galparsoro, I., Connor, D.W., Borja, A., Aish, A., Amorim, P., Bajjouk, T., Chambers, C., Coggan, R., Dirberg, G., Ellwood, H., Evans, D., Goodin, K.L., Grehan, A., Haldin, J., Howell, K., Jenkins, C., Michez, N., Mo, G., Buhl-Mortensen, P., Pearce, B., Populus, J., Salomidi, M., Sánchez, F., Serrano, A., Shumchenia, E., Tempera, F., Vasquez, M., 2012. Using EUNIS habitat classification for benthic mapping in European seas: Present concerns and future needs. *Mar. Pollut. Bull.* 64 (12), 2630–2638.
- Grothe, O., Schieders, J., 2011. Spatial dependence in wind and optimal wind power allocation: A copula-based analysis. *Energy Policy* 39 (9), 4742–4754. <https://doi.org/10.1016/j.enpol.2011.06.052>.
- Heip, C.H.R., Basford, D., Craeymeersch, J.A., Dewarumez, J.-M., de Wilde, P., Dörjes, J., Duineveld, G., Eleftheriou, A., Herman, P.M.J., Huys, R., Irion, G., Niermann, U., Kingston, P., Künitzer, A., Rachor, E., Rumohr, H., Soetaert, K., Soltwedel, T., 1992. The benthic communities of the North Sea: A summary of the results of the North Sea benthos survey. *ICES Coop. Res. Report.* 190, 148–175.
- Hewitt, J.E., Wang, D., Francis, M., Lundquist, C., Duffy, C., Schoeman, D., 2015. Evaluating demersal fish richness as a surrogate for epibenthic richness in management and conservation. *Divers. Distrib.* 21 (8), 901–912. <https://doi.org/10.1111/ddi.12336>.
- Hiddink, J.G., Jennings, S., Kaiser, M.J., Queirós, A.M., Duplisea, D.E., Piet, G.J., 2006. Cumulative impacts of seabed trawl disturbance on benthic biomass, production, and species richness in different habitats. *Can. J. Fish. Aquat. Sci.* 63 (4), 721–736. <https://doi.org/10.1139/f05-266>.
- Hiddink, J.G., Jennings, S., Sciberras, M., Szostek, C.L., Hughes, K.M., Ellis, N., Rijnsdorp, A.D., McConnaughey, R.A., Mazor, T., Hilborn, R., Collie, J.S., Pitcher, C.R., Amoroso, R.O., Parma, A.M., Suuronen, P., Kaiser, M.J., 2017. Global analysis of depletion and recovery of seabed biota after bottom trawling disturbance. *Proc. Natl. Acad. Sci.* 114 (31), 8301–8306. <https://doi.org/10.1073/pnas.1618858114>.
- Hiddink, J.G., Jennings, S., Sciberras, M., Bolam, S.G., Cambiè, G., McConnaughey, R.A., Mazor, T., Hilborn, R., Collie, J.S., Pitcher, C.R., Parma, A.M., Suuronen, P., Kaiser, M.J., Rijnsdorp, A.D., Trenkel, V., 2019. Assessing bottom trawling impacts based on the longevity of benthic invertebrates. *J. Appl. Ecol.* 56 (5), 1075–1084. <https://doi.org/10.1111/1365-2664.13278>.
- Hijmans, R.J., Phillips, S., Leatherick, J., Elith, J., 2017. Dismo: Species distribution modelling.
- Huang, Z., Brooke, B.P., Harris, P.T., 2011. A new approach to mapping marine benthic habitats using physical environmental data. *Cont. Shelf Res.* 31 (2), S4–S16. <https://doi.org/10.1016/j.csr.2010.03.012>.
- ICES, 2009. Manual for the offshore Beam Trawl Surveys. Working Group on Beam Trawl Surveys.
- ICES, 2019b. Interim Report of the Working Group on Fisheries Benthic Impact and Trade-offs (WGFBIT), 12–16 November 2018. ICES Headquarters, Copenhagen, Denmark.
- ICES, 2020. Working Group on Fisheries Benthic Impact and Trade-Offs (WGFBIT). outputs from 2019 meeting). ICES Scientific Reports.
- ICES, 2019a. Working Group on Marine Habitat Mapping (WGMHM), ICES Scientific Reports. <https://doi.org/10.17895/ices.pub.5578>.
- Johnson, C.N., Balmford, A., Brook, B.W., Buettel, J.C., Galetti, M., Guangchun, L., Wilmschurst, J.M., 2017. Biodiversity losses and conservation responses in the Anthropocene. *Science* (80-. 356 (6335), 270–275. <https://doi.org/10.1126/science.am9317>.

- Jones, C.G., Lawton, J.H., Shachak, M., 1994. Organisms as ecosystem engineers. *Oikos* 69 (3), 373. <https://doi.org/10.2307/3545850>.
- Jørgensen, L.L., Renaud, P.E., Cochran, S.K.J., 2011. Improving benthic monitoring by combining trawl and grab surveys. *Mar. Pollut. Bull.* 62 (6), 1183–1190. <https://doi.org/10.1016/j.marpolbul.2011.03.035>.
- Kaiser, M.J., Ramsay, K., Richardson, C.A., Spence, F.E., Brand, A.R., 2000. Chronic fishing disturbance has changed shelf sea benthic community structure. *J. Anim. Ecol.* 69 (3), 494–503. <https://doi.org/10.1046/j.1365-2656.2000.00412.x>.
- Kaiser, M.J., Hilborn, R., Jennings, S., Amaroso, R., Andersen, M., Balliet, K., Barratt, E., Bergstad, O.A., Bishop, S., Boström, J.L., Boyd, C., Bruce, E.A., Burden, M., Carey, C., Clermont, J., Collie, J.S., Delahunty, A., Dixon, J., Eayrs, S., Edwards, N., Fujita, R., Gauvin, J., Gleason, M., Harris, B., He, P., Hiddink, J.G., Hughes, K.M., Inostroza, M., Kenny, A., Kritzer, J., Rijnsdorp, A.D., Rillat, S., Rodmell, D.P., Rose, C., Sethi, S.A., Masters, J., Mazar, T., McConnaughey, R.A., Moenne, M., Francis, Nimick, A.M., Olsen, A., Parker, D., Parma, A., Penney, C., Pierce, D., Pitcher, R., Pol, M., Richardson, E.D., Rijnsdorp, A.D., Rillat, S., Rodmell, D.P., Rose, C., Sethi, S.A., Short, K., Suuronen, P., Taylor, E., Wallace, S., Webb, L., Wickham, E., Wilding, S.R., Wilson, A., Winger, P., Sutherland, W.J., 2016. Prioritization of knowledge-needs to achieve best practices for bottom trawling in relation to seabed habitats. *Fish Fish.* 17 (3), 637–663. <https://doi.org/10.1111/faf.12134>.
- Kröncke, I., Reiss, H., Eggleton, J.D., Aldridge, J., Bergman, M.J.N., Cochran, S., Craeymeersch, J.A., Degraer, S., Desroy, N., Dewarumez, J.-M., Duineveld, G.C.A., Essink, K., Hillewaert, H., Lavaleye, M.S.S., Moll, A., Nehring, S., Newell, R., Oug, E., Pohlmann, T., Rachor, E., Robertson, M., Rumohr, H., Schratzberger, M., Smith, R., Berghe, E.V., van Dalen, J., van Hoey, G., Vincx, M., Willems, W., Rees, H.L., 2011. Changes in North Sea macrofauna communities and species distribution between 1986 and 2000. *Estuar. Coast. Shelf Sci.* 94 (1), 1–15. <https://doi.org/10.1016/j.ecss.2011.04.008>.
- Kunitzer, A., Basford, D., Craeymeersch, J.A., Dewarumez, J.M., Dorjes, J., Duineveld, G.C.A., Eleftheriou, A., Heip, C., Herman, P., Kingston, P., Niermann, U., Rachor, E., Rumohr, H., de Wilde, P.A.J., 1992. The benthic infauna of the North Sea: Species distribution and assemblages. *ICES J. Mar. Sci.* 49 (2), 127–143. <https://doi.org/10.1093/icesjms/49.2.127>.
- Lecours, V., Devillers, R., Schneider, D.C., Lucieer, V.L., Brown, C.J., Edinger, E.N., 2015. Spatial scale and geographic context in benthic habitat mapping: Review and future directions. *Mar. Ecol. Prog. Ser.* 535, 259–284. <https://doi.org/10.3354/meps11378>.
- Linderman, M., 2013. Rclusterpp: Linkable C++ clustering.R package version 0.2.3.
- McArthur, M.A., Brooke, B.P., Przeslawski, R., Ryan, D.A., Lucieer, V.L., Nichol, S., McCallum, A.W., Mellin, C., Cresswell, I.D., Radke, L.C., 2010. On the use of abiotic surrogates to describe marine benthic biodiversity. *Estuar. Coast. Shelf Sci.* 88 (1), 21–32. <https://doi.org/10.1016/j.ecss.2010.03.003>.
- Menge, B.A., Sutherland, J.P., 1976. Species diversity gradients: Synthesis of the roles of predation, competition, and temporal heterogeneity. *Am. Nat.* 110 (973), 351–369. <https://doi.org/10.1086/283073>.
- Millar, C., Large, S., Magnusson, A., 2019. icesDatras: DATRAS trawl survey database web services.
- Oksanen, J., Blanchet, F.G., Friendly, M., Kindt, R., Legendre, P., McGlinn, D., Minchin, P.R., O'Hara, B., Simpson, G.L., Solymos, P., Henry, M., Stevens, H., Szoecs, E., Wagner, H., 2019. Vegan: Community ecology package.R package version 2.5-6.
- Rees, H.L., Eggleton, J.D., Rachor, E., Vanden Berghe, E., 2007. Structure and dynamics of the North Sea benthos. ICES Cooperative Research Report No. 288.
- Reiss, H., Degraer, S., Duineveld, G.C.A., Kröncke, I., Aldridge, J., Craeymeersch, J.A., Eggleton, J.D., Hillewaert, H., Lavaleye, M.S.S., Moll, A., Pohlmann, T., Rachor, E., Robertson, M., Vanden Berghe, E., van Hoey, G., Rees, H.L., 2010. Spatial patterns of infauna, epifauna, and demersal fish communities in the North Sea. *ICES J. Mar. Sci.* 67, 278–293. <https://doi.org/10.1093/icesjms/ftp253>.
- Reiss, H., Birchenough, S., Borja, A., Buhl-mortensen, L., Craeymeersch, J., Dannheim, J., Darr, A., Galparsoro, I., Gogina, M., Neumann, H., Populus, J., Rengstorf, A.M., Valle, M., Hoey, G.V., Zettler, M.L., Degraer, S., 2015. Benthos distribution modelling and its relevance for marine ecosystem management. *ICES J. Mar. Sci.* 72, 297–315. <https://doi.org/10.1093/icesjms/fsu107> Review.
- Rijnsdorp, A.D., Bolam, S.G., Garcia, C., Hiddink, J.G., Hintzen, N.T., van Denderen, P.D., van Kooten, T., 2018. Estimating sensitivity of seabed habitats to disturbance by bottom trawling based on the longevity of benthic fauna. *Ecol. Appl.* 28 (5), 1302–1312. <https://doi.org/10.1002/eap.2018.28.issue-510.1002/eap.1731>.
- Roland Pitcher, C., Lawton, P., Ellis, N., Smith, S.J., Inceze, L.S., Wei, C.-L., Greenlaw, M.E., Wolff, N.H., Sameoto, J.A., Snelgrove, P.V.R., 2012. Exploring the role of environmental variables in shaping patterns of seabed biodiversity composition in regional-scale ecosystems. *J. Appl. Ecol.* 49 (3), 670–679. <https://doi.org/10.1111/j.1365-2664.2012.02148.x>.
- Rubidge, E.M., Gale, K.S.P., Curtis, J.M.R., 2016. Community ecological modelling as an alternative to physiographic classifications for marine conservation planning. *Biodivers. Conserv.* 25 (10), 1899–1920. <https://doi.org/10.1007/s10531-016-1167-x>.
- Sardain, A., Sardain, E., Leung, B., 2019. Global forecasts of shipping traffic and biological invasions to 2050. *Nat. Sustain.* 2 (4), 274–282. <https://doi.org/10.1038/s41893-019-0245-y>.
- Schiele, K.S., Darr, A., Zettler, M.L., 2014. Verifying a biotope classification using benthic communities - An analysis towards the implementation of the European Marine Strategy Framework Directive. *Mar. Pollut. Bull.* 78 (1-2), 181–189. <https://doi.org/10.1016/j.marpolbul.2013.10.045>.
- Smoliński, S., Radtke, K., 2017. Spatial prediction of demersal fish diversity in the Baltic Sea: Comparison of machine learning and regression-based techniques. *ICES J. Mar. Sci.* 74, 102–111. <https://doi.org/10.1093/icesjms/fsw136>.
- Stephens, D., 2015. North Sea and UK shelf substrate composition predictions, with links to GeoTIFFs. <https://doi.org/10.1594/PANGAEA.845468>.
- Stephens, David, Diesing, Marcus, 2015. Towards quantitative spatial models of seabed sediment composition. *PLoS ONE* 10 (11), e0142502. <https://doi.org/10.1371/journal.pone.0142502>.
- Stevens, T., Connolly, R.M., 2004. Testing the utility of abiotic surrogates for marine habitat mapping at scales relevant to management. *Biol. Conserv.* 119 (3), 351–362. <https://doi.org/10.1016/j.biocon.2003.12.001>.
- Strong, J.A., Clements, A., Lillis, H., Galparsoro, I., Bildstein, T., Pesch, R., 2019. A review of the influence of marine habitat classification schemes on mapping studies: Inherent assumptions, influence on end products, and suggestions for future developments. *ICES J. Mar. Sci.* 76, 10–22. <https://doi.org/10.1093/icesjms/fsy161>.
- Turner, R., 2019. Deldir: Delaunay Triangulation and Dirichlet (Voronoi) Tessellation.
- van Denderen, P.D., Bolam, S.G., Hiddink, J.G., Jennings, S., Kenny, A., Rijnsdorp, A.D., van Kooten, T., 2015. Similar effects of bottom trawling and natural disturbance on composition and function of benthic communities across habitats. *Mar. Ecol. Prog. Ser.* 541, 31–43. <https://doi.org/10.3354/meps11550>.
- van der Reijden, K.J., Hintzen, N.T., Govers, L.L., Rijnsdorp, A.D., Olf, H., Paiva, V.H.R., 2018. North Sea demersal fisheries prefer specific benthic habitats. *PLoS ONE* 13 (12), e0208338. <https://doi.org/10.1371/journal.pone.0208338>.
- Vasquez, M., Mata Chacón, D., Tempera, F., O'Keefe, E., Galparsoro, I., Sanz Alonso, J.L., Gonçalves, J.M.S., Bentes, L., Amorim, P., Henriques, V., McGrath, F., Monteiro, P., Mendes, B., Freitas, R., Martins, R., Populus, J., 2015. Broad-scale mapping of seafloor habitats in the north-east Atlantic using existing environmental data. *J. Sea Res.* 100, 120–132. <https://doi.org/10.1016/j.seares.2014.09.011>.
- Verfaillie, E., Degraer, S., Schelfaut, K., Willems, W., Van Lancker, V., 2009. A protocol for classifying ecologically relevant marine zones, a statistical approach. *Estuar. Coast. Shelf Sci.* 83 (2), 175–185. <https://doi.org/10.1016/j.ecss.2009.03.003>.
- White, C., Halpern, B.S., Kappel, C.V., 2012. Ecosystem service tradeoff analysis reveals the value of marine spatial planning for multiple ocean uses. *Proc. Natl. Acad. Sci. U. S. A.* 109 (12), 4696–4701. <https://doi.org/10.1073/pnas.1114215109>.